RSC Advances

ROYAL SOCIETY OF CHEMISTRY

www.rsc.org/advances

RSC Advances

RSCPublishing

COMMUNICATION

A Non-Micellar Synthesis of Mesoporous Carbon via Spinodal Decomposition

Cite this: DOI: 10.1039/x0xx00000x

Kimberly M Nelson,[a] Zhen-An Qiao,[b] Shannon M. Mahurin,[b] Richard T. Mayes,[b] Craig A. Bridges,[b] and Sheng Dai *[ab]

Received 00th January 2012,
Accepted 00th January 2012

DOI: 10.1039/x0xx00000x

www.rsc.org/

Mesoporous carbons were prepared via spinodal decomposition of non-amphiphilic linear polyethylene glycol with phloroglucinol-formaldehyde resin under refluxing acidic ethanol conditions. By shifting the molecular weight and the concentration of polyethylene glycol, both mesopore size and volume can be tuned, respectively.

Traditional porous carbon materials are derived from coal, wood, biomass, or polymers.[1] These carbons are typically microporous, which are formed from defects left by heteroatoms that are eliminated during carbonization. Microporous carbons are often inadequate in reference to conductivity, mass transport, and structural integrity due to remaining heteroatoms, restricted flow pathways, and lack of structural control. These deficiencies can be resolved by the introduction of mesoporosity, which make them ideal for catalysis, batteries, supercapacitors, and adsorbents.[2] Mesoporous carbons that can be tailored to optimize these applications are in high demand.

The standard templating synthesis uses methods that can be both costly and hazardous on the industrial scale.[2a] For instance, hard-templating of mesoporous carbons involves using a sacrificial silica template in combination with a carbon precursor, in which the template is etched after carbonization with harsh acids or bases (i.e. HF, NaOH) and a carbon inverse replica is revealed.[3] Soft-templating synthesis tends to be less severe and is based on a self-assembly approach using block copolymer templating agents, which are removed via calcination.[4] The block copolymer can be synthetically intensive to produce, making them very costly. While both of these methods produce well-defined mesopore size distributions and morphologies, they lack a facile route for mesopore development and a cost effective porogen that is relinquished by the process for industrial scale viability. Recently Seo and Hillmyer demonstrated polymerization induced microphase separation of trithiocarbonate terminated polylactide with vinylbenzene/divinylbenzene for mesoporous polymer synthesis via radical addition-fragmentation chain transfer.[5] Polymerization quenched spinodal decomposition creates mesoscopic domains and, when combined with carbonization, the pore forming polymer is effectively removed while the carbon precursor remains, preserving the mesostructure.

Herein, we establish a surfactant-free preparation of mesoporous carbon through the in-situ polymerization of phloroglucinol-formaldehyde (PF) resins in the presence of polyethylene glycol (PEG) in acidic ethanol under reflux. The acid catalysed condensation polymerization of PF resins have served as a carbon precursor previously[6] but the essence of our methodology resides in the synthesis of mesoporous carbon through spinodal decomposition instead of traditional micellar self-assembly approaches.[6a] In lieu of triblock copolymers as

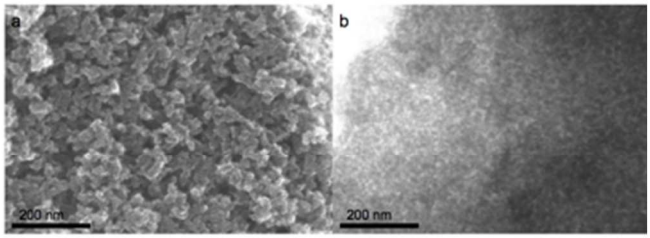

Figure 1 SEM (a) and TEM image (b) of mesoporous carbon from prepared PF-PEG (14 k MW) precursor.

[a] *Department of Chemistry, University of Tennessee, Knoxville, Tennessee 37996, USA.*

[b] *Chemical Sciences Division, Oak Ridge National Laboratory, Oak Ridge, Tennessee 37831 USA, Email: dais@orl.gov; Fax: +1-865-576-5235;Tel: +1-865-576-7307*

† Electronic supplementary information (ESI) available: Experimental details including synthesis of PEG templated phloroglucinol-formaldehyde derived carbon, associated SEM/TEM characterization, and SAXS analysis.

templating agents, utilization of linear PEG

Table 1 Nitrogen adsorption properties of mesoporous carbons varying MW of PEG template

PEG MW [Da]	S_{BET} [m^2 g^{-1}][a]	V_{total} [cm^3 g^{-1}]	V_{meso} [cm^3 g^{-1}][b]	D_{meso} [nm][c]
2 k	360	0.197	0.098 (49.7)	9
4 k	368	0.356	0.267 (75.0)	14
8 k	372	0.480	0.395 (82.3)	16
14 k	321	0.637	0.571 (89.6)	25
20 k	368	0.374	0.285 (76.2)	25
100 k	375	0.746	0.677 (91.2)	31
200 k	375	0.629	0.558 (88.7)	21

a) Specific surface area calculated using the BET equation in the relative pressure range of 0.05-0.20. b) The number in parentheses are percentages of mesopore volume out of total pore volume. c) Average pore diameter found at maximum differential pore volume.

provides a more cost effective alternative as a sacrificially templating agent.

In a typical run, phloroglucinol, formaldehyde, and PEG were mixed in ethanol under acidic conditions [see the Supporting information]. Under refluxing conditions, PF-PEG aggregates were formed and precipitated. The PF-PEG solid was then dried and carbonized at 850 °C for 2 h under Ar atmosphere at a rate of 2 °C/min. Under these conditions, the near complete degradation of all MWs of PEG used can be achieved and carbonization of remaining PF at this temperature could yield a material optimal for conductivity testing.[7] The mesoporosity of the resulting carbon material was confirmed via scanning electron microscopy (SEM) and transmission electron microscopy (TEM) (Fig. 1 and Figures S1 – S8 in SI). The surface area of these materials was measured using nitrogen adsorption (Fig.2).

On the basis of our results and literature reports, a possible mechanism for the formation of mesoporosity under the specified conditions is summarized in Scheme 1. Upon addition of formaldehyde, acid catalyzed PF condensation polymerization occurs. As step- growth polymerization proceeds, the hydrophilic PF macromolecules undergo hydrogen-bonding interactions with the PEG polymers, leading to the formation of homogeneous PF-PEG aggregates, i.e. "polymer blend". As PF molecular weight increases, microphase separation of the aforementioned

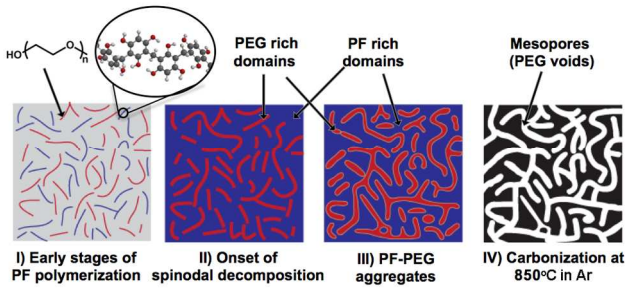

Scheme 1 Schematic illustration of spinodal decomposition (I to III) and subsequent formation of mesoporous carbon (IV) from PF-PEG adduct.

homogeneous

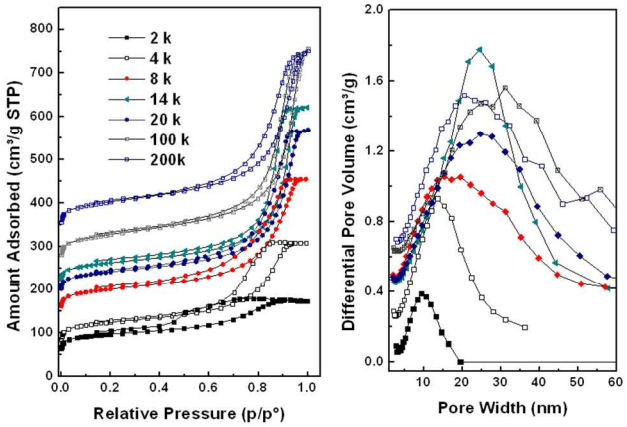

Fig. 2 Nitrogen -196 °C adsorption isotherms (left) and corresponding pore size distributions (right) calculated using KJS method of carbon samples with respective PEG (in Da). For clarity, the isotherms were offset by consecutive increments of 50 cm^3/g and pore size distributions offset in consecutive increments of 0.2 cm^3/g.

aggregates into the mesoscopic domains via spinodal decomposition is evidenced by the co-continuous structure found in Figure 1 and only microporosity in the PF sample without PEG addition (Figure S10 in SI).[16] The PF polymerization "chemically quenches" the reaction in the spinodal region and as the phase composition changes and new phase miscibility conditions are established for the newly formed polymer-polymer blend.

The acid is an essential component not only to the catalyzed polymerization of PF polymers but also to the interaction between the PF-PEG for driving the spinodal decomposition. The latter was evidenced by the formation of only microporous carbons from the samples prepared without acid (Figure S10 in SI). Acidic ethanol at increased temperature reduces polymer-polymer interactions, causing the end-to-end distance of the polymer chains to shrink. Eventually cluster formation becomes favourable as polymer chains collapse, leading to efficient spinodal decomposition.[8] The as- synthesized material is non-porous (Figure S10 in SI) after drying and curing. The subsequent carbonization at 850 °C under inert Ar atmosphere destabilizes and decomposes the high oxygen containing PEG revealing an inverse carbon replica. The mesoporosity is evident from the condensation step in the nitrogen adsorption isotherm with desorption hysteresis characteristics of the type IV isotherm in Figure 2. Textural analysis was done using the Barrett, Joyner, and Halenda (BJH) method to calculate the pore size distributions according to the Kruk, Jaroniec, and Sayari (KJS) method, specific surface area using the Brunauer, Emmett, and Teller (BET) method, and micropore surface area and volume using the *t-plot* given in Table 1 and Table 2.[9] In comparison, carbon produced at 850 °C using a similar procedure but with the triblock copolymer template, Pluronic F127 (MW 12.6 kDa, $PEO_{106}PPO_{70}PEO_{106}$), produced a similar micro- mesopore ratio and pore volume but with an average pore size of 8.9 nm and a BET surface area of 518 m^2/g.[10] Although the pore size

distribution for PF-PEG (14 kDa) covers a much wider range of mesoporosity than that of Pluronic F127 templated PF resin,

Table 2 Nitrogen adsorption properties of mesoporous carbons varying concentration of PEG template.

PEG Conc. [mM] [a]	S_{BET} [$m^2 g^{-1}$] [b]	S_{meso} [$m^2 g^{-1}$] [c]	V_{Total} [$cm^3 g^{-1}$] [d]	V_{meso} [$cm^3 g^{-1}$] [e]	D_{meso} [nm] [f]
2.9	392	83	0.244	0.121 (49.6)	19
1.4	321	164	0.546	0.481 (88.1)	25
0.63	321	159	0.637	0.571 (89.6)	16

[a] Phloroglucinol to 14 kDa PEG weight ratio. [b] Specific surface area calculated using the BET equation in the relative pressure range of 0.05-0.20; [c,d] Mesopore and external surface area. [e] The numbers in parentheses are percentages of mesopore volume out of total pore volume. [f] Average pore diameter found at maximum differential pore volume.

the adsorbed N_2 contribution from micropores is only 0.066 cm^3/g compared to 0.12 cm^3/g, attributing nearly 90 % of the pore volume to mesopores in contrast to 81 %, respectively.

Under acidic ethanol reflux conditions, linear PEG chains agglomerate via spinodal decomposition in a similar fashion to the self-assembly of hydrophobic and hydrophilic blocks of Pluronic F127. In the Pluronic F127 templated carbon, variation in mesopore size, pore size distribution discrepancies, and increased microporosity is due to self-assembly of micelles during the reflux and curing process. The hydrogen bonding between the PF resin and PEO corona yields the high microporosity in the resulting carbon; in contrast, PF resin has a much stronger interaction with the exterior of the PEG, owing to the separate polymer phases.

As seen in Table 1, mesoporosity extends to carbon produced using this method along a molecular weight range of 2 to 200 kDa PEG. Below 2 kDa PEG, no mesoporosity was observed and microporosity was nominal (Figure S10 in SI). At 2 kDa PEG, the desorption hysteresis closes at ~0.45 P/P_o, which is typically due to cavitation in spherical pores. The small-angle X-ray scattering (SAXS) patterns of as-synthesized samples in Figure S11 consist of one broad diffraction peak with *q* values of 0.092 - 0.17, and no resolved features are observed for higher reflections. This result suggests a worm-like mesopore dominated structure, which agrees well with the results observed from TEM images. When reviewing the pore size distribution from the carbon sample using the upper most MW PEG, it is apparent that the broad pore size distribution is not a desirable characteristic for templated materials; although, this still provides a reasonably large effective range. The observed results in Fig. 2 confirmed that by shifting the molecular weight from low to high, the average pore size increases. These values, however, cannot be reflected in the BJH average pore size calculation, as this method is used for mesopores in the range of 2 to 50 nm. With the pore size distributions for the larger molecular weight PEG, the calculation is not valid as it reaches this limit, considering the values fall well into macropore domain.

The mesopore volume can then be adjusted through the concentration of PEG in solution. This approach allows the

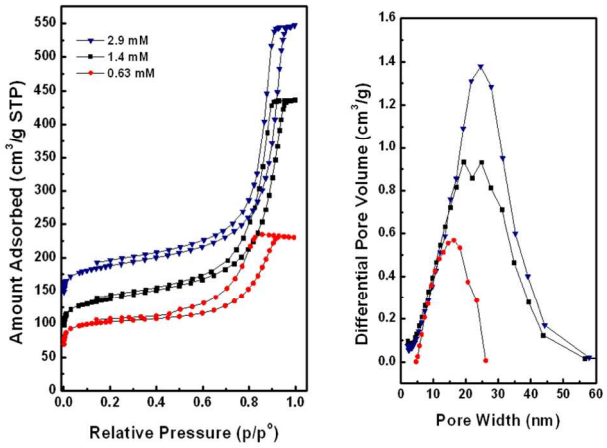

Fig. 3 Nitrogen -196 °C adsorption isotherms (left) and corresponding pore size distributions (right) calculated using BJH method of carbon samples with respective PEG (MW = 14 k Da) concentration. For clarity, the isotherms were offset consecutively by increments of 50 cm^3/g.

mesopore volume of the resulting carbon to be either raised or lowered, as shown in Fig. 3, for a specific application. Reducing the concentration from 2.9 mM to 1.4 mM PEG results in a minimal shift in pore size indicating, in this case, that the concentration determines the amount of the corresponding polymer phase. In contrast, when the amount of PEG is further reduced to 0.63 mM, the microporosity of the sample is doubled and mesoporosity is reduced by nearly 40 % (Table 2). By the reversal in porosity, decreasing the concentration of PEG shifts the composition ratio towards the binodal near a metastable region.[11] Consequently, there is less defined spinodal decomposition occurring and fractal clusters are formed that generate the mesopores and micropores, respectively.[12]

In summary, using nonsurfactant linear PEG as a template for mesoporous carbon is reported. In contrast to prior soft templating approaches to mesoporous carbon, tailoring is limited only to the MW selection available. This material shows improvement by reducing inherent microporosity while increasing pore size. By tuning the PF to PEG ratio, the mesopore volume can also be adjusted. These characteristics may be useful where mesoporosity is necessary for mass transport. Increased adsorption sites can be added using various means of activation to increase microporosity and add functionality.[10, 13] The ability to finely tune the mesoporosity of a carbon material through molecular weight and concentration of PEG is relevant due to the novelty, particularly in comparison to traditionally triblock copolymer templates where tuning would require complex and complex polymer synthesis. This concept is especially important for industrial scale synthesis.

This work was fully sponsored by the Division of Chemical Sciences, Geosciences, and Biosciences, Office of Basic Energy Sciences, U.S. Department of Energy.

Notes and references

1 a) C. Liang, Z. Li and S. Dai, *Angew. Chem., Int. Ed.*, 2008, **47**, 3696-3717; b) R. L. Tseng and S. K. Tseng, *J. Colloid Interface Sci.*, 2005, **287**, 428-437; c) R. J. White, V. Budarin, R. Luque, J. H. Clark and D. J. Macquarrie, *Chem. Soc. Rev.*, 2009, **38**, 3401-3418.

2 a) Y. Shi, Y. Wan and D. Zhao, *Chem. Soc. Rev.*, 2011, **40**, 3854; b) Y. P. Zhai, Y. Q. Dou, D. Y. Zhao, P. F. Fulvio, R. T. Mayes and S. Dai, *Adv. Mater.*, 2011, **23**, 4828-4850.

3 a) A. H. Lu and F. Schüth, *Adv. Mater.*, 2006, **18**, 1793-1805; b) R. Ryoo, S. H. Joo and S. Jun, *J. Phys. Chem. B*, 1999, **103**, 7743-7746; c) S. Jun, S. H. Joo, R. Ryoo, M. Kruk, M. Jaroniec, Z. Liu, T. Ohsuna and O. Terasaki, *J. Am. Chem. Soc.*, 2000, **122**, 10712-10713.

4 a) C. Liang and S. Dai, in *J. Am. Chem. Soc.*, 2006, vol. 128, pp. 5316-5317; b) Y. Meng, D. Gu, F. Zhang, Y. Shi, L. Cheng, D. Feng, Z. Wu, Z. Chen, Y. Wan, A. Stein and D. Zhao, *Chem. Mater.*, 2006, **18**, 4447-4464; c) Y. Meng, D. Gu, F. Q. Zhang, Y. F. Shi, H. F. Yang, Z. Li, C. Z. Yu, B. Tu and D. Y. Zhao, *Angew. Chem., Int. Ed.*, 2005, **44**, 7053-7059; d) C. D. Liang, K. L. Hong, G. A. Guiochon, J. W. Mays and S. Dai, *Angew. Chem., Int. Ed.*, 2004, **43**, 5785-5789.

5 M. Seo and M. A. Hillmyer, *Science*, 2012, **336**, 1422-1425.

6 a) C. D. Liang and S. Dai, *Chem. Mater.*, 2009, **21**, 2115-2124; b) S. Tanaka, N. Nakatani, A. Doi and Y. Miyake, *Carbon*, 2011, **49**, 3184-3189; c) T. Y. Ma, L. Liu and Z. Y. Yuan, *Chem. Soc. Rev.*, 2013, **42**, 3977-4003.

7 a) N. S. Vrandecic, M. Erceg, M. Jakic and I. Klaric, *Thermochim. Acta*, 2010, **498**, 71-80; b) F. Y. Wang, C. C. M. Ma and W. J. Wu, *J. Appl. Polym. Sci.*, 2001, **80**, 188-196.

8 a) B. Hammouda, D. L. Ho and S. Kline, *Macromolecules*, 2004, **37**, 6932-6937; b) P. Pang and P. Englezos, *Colloids Surf., A*, 2002, **204**, 23-30; c) B. Briscoe, P. Luckham and S. Zhu, *J. Appl. Polym. Sci.*, 1998, **70**, 419-429; d) A. Mehrdad and R. Akbarzadeh, *J. Chem. Eng. Data*, 2010, **55**, 2537-2541.

9 a) M. Kruk and M. Jaroniec, *Chem. Mat.*, 2001, **13**, 3169-3183; b) M. Kruk, M. Jaroniec and A. Sayari, *Langmuir*, 1997, **13**, 6267-6273.

10 X. Wang, J. S. Lee, C. Tsouris, D. W. DePaoli and S. Dai, in *J. Mater. Chem.*, 2010, vol. 20, pp. 4602-4607.

11 T. Norisuye, M. Takeda and M. Shibayama, *Macromolecules*, 1998, **31**, 5316-5322.

12 K. Binder, *Colloid. Polym. Sci.*, 1987, **265**, 273-288.

13 Z. Zhang, M. Xu, H. Wang and Z. Li, *Chem. Eng. J.*, 2010, **160**, 571-577.

